2-P

NASA CR 134644

IMPROVING IMPACT RESISTANCE OF CERAMIC MATERIALS BY ENERGY ABSORBING SURFACE LAYERS

By H. P. Kirchner and J. Seretsky

Ceramic Finishing Company
Box 498
State College, Pennsylvania 16801

Prepared for
National Aeronautics and Space Administration

NASA—Lewis Research Center
Contract NAS3—17765

(NASA-CR-134644) IMPROVING IMPACT RESISTANCE OF CERAMIC MATERIALS BY ENERGY ABSORBING SURFACE LAYERS (Ceramic Finishing Co.) 56 p HC $6.00 CSCL 11D

N74-31024

Unclas
G3/18 45738

1. Report No.	2. Government Accession No.	3. Recipient's Catalog No.
NASA CR 134644		

4. Title and Subtitle	5. Report Date
IMPROVING IMPACT RESISTANCE OF CERAMIC MATERIALS BY ENERGY ABSORBING SURFACE LAYERS	March, 1974
	6. Performing Organization Code
7. Author(s)	8. Performing Organization Report No.
H. P. Kirchner and J. Seretsky	
	10. Work Unit No.
9. Performing Organization Name and Address	YOA5935
Ceramic Finishing Company P. O. Box 498 State College, Pennsylvania 16801	11. Contract or Grant No.
	NAS3-17765
	13. Type of Report and Period Covered
12. Sponsoring Agency Name and Address	Contractor Report
National Aeronautics & Space Administration Washington, D. C. 20546	14. Sponsoring Agency Code

15. Supplementary Notes

Project Manager, J. R. Johnston
Lewis Research Center, Cleveland, Ohio 44135

16. Abstract

Energy absorbing surface layers were used to improve the impact resistance of silicon nitride and silicon carbide ceramics. Low elastic modulus materials were used. In some cases, the low elastic modulus was achieved using materials that form localized microcracks as a result of thermal expansion anisotropy, thermal expansion differences between phases, or phase transformations. In other cases, semi-vitreous or vitreous materials were used. Substantial improvements in impact resistance were observed at room and elevated temperatures.

17. Key Words (Suggested by Author(s))		18. Distribution Statement
silicon nitride	elastic modulus	
silicon carbide	impact resistance	
magnesium dititanate	phase transformation	
petalite	vitreous materials	Unclassified
thermal expansion	surface treatments	
thermal expansion anisotropy	energy absorbing surfaces	

19. Security Classif. (of this report)	20. Security Classif. (of this page)	21. No. of Pages	22. Price*
Unclassified	Unclassified	54 60	$3.00

* For sale by the National Technical Information Service, Springfield, Virginia 22151

NASA-C-168 (Rev. 6-71)

TABLE OF CONTENTS

		Page
	Title Page	i
	List of Tables	iv
	List of Figures	vi
I.	Summary	1
II.	Introduction	2
III.	Procedures	5
	A. Materials	5
	B. Specimen Fabrication	8
	C. Treatments	8
	D. Impact Testing	14
	E. Characterization	14
IV.	Results and Discussion	16
	A. Impact Resistance of Control Specimens	16
	B. Surfaces with Microcracks Caused by Thermal Expansion Anisotropy	21
	C. Surfaces with Microcracks Caused by Thermal Expansion Differences Between Two Phases	30
	D. Surfaces with Microcracks Caused by a Phase Transformation	33
	E. Vitreous or Semi-Vitreous Surfaces	34
	F. Other Surface Treatments	47
V.	Conclusions	51
VI.	References	52

LIST OF TABLES

Page

I. Impact Resistance of Norton NC-132 Silicon Nitride. 17

II. Impact Resistance of Norton Silicon Nitride Control Specimens. 18

III. Impact Resistance of AVCO Silicon Nitride Control Specimens. 19

IV. Impact Resistance of Norton NC-203 Silicon Carbide at Various Temperatures. 22

V. Impact Resistance of Norton NC-203 Silicon Carbide Control Specimens. 24

VI. Impact Resistance of Norton HS-130 Silicon Nitride Bars with Cemented Plates of Magnesium Dititanate 25

VII. Impact Resistance of AVCO Silicon Nitride Bars with Cemented Plates of Magnesium Dititanate 27

VIII. Impact Resistance of AVCO Silicon Nitride with Hot Pressed $MgTi_2O_5$ Surface Layers 29

IX. Impact Resistance of Norton NC-203 Silicon Carbide with Hot Pressed Si_3N_4-SiC Surface Layers 32

X. Impact Resistance of AVCO Silicon Nitride with Cemented Plates of Zirconia 35

XI. Impact Resistance of Norton NC-203 Silicon Carbide with Vitreous Surface Layers 37

XII. Elevated Temperature Impact Resistance of AVCO Silicon Nitride with Vitreous Surface Layers 38

LIST OF TABLES (continued)

		Page
XIII.	Elevated Temperature Impact Resistance of Norton NC-203 Silicon Carbide with Vitreous Surface Layers.	39
XIV.	Elevated Temperature Impact Resistance of Norton NC-203 Silicon Carbide with Petalite Treatment	41
XV.	Impact Resistance of Norton HS-130 Silicon Nitride Treated with G-24 Frit	46
XVI.	Flexural Strength of Norton Silicon Nitride Packed in Various Powders.	48
XVII.	Impact Resistance of Norton Silicon Nitride Packed in Various Powders.	50

LIST OF FIGURES

		Page
1.	Microstructure of Hot Pressed Norton NC-132 Silicon Nitride.	6
2.	Microstructure of Hot Pressed Norton NC-203 Silicon Carbide.	7
3.	Fracture Surface of Magnesium Dititanate, as Hot Pressed, Ten Micrometer Average Grain Size.	10
4.	Impact Test Specimen with Cemented Magnesium Dititanate Plate.	21
5.	Hot Pressed Magnesium Dititanate on AVCO Silicon Nitride	28
6.	Impact Resistance vs. Temperature for Norton NC-203 Silicon Carbide	42
7.	Surface of AVCO Silicon Nitride Specimen with Petalite Surface, after Impact Testing	43
8.	AVCO Silicon Nitride Burner Rig Specimens with Petalite Surfaces.	44

I. SUMMARY

The following types of energy absorbing surface layers were formed on silicon nitride and silicon carbide ceramics:

1. Surface layers with microcracks formed as a result of thermal expansion anisotropy.
2. Surface layers with microcracks formed as a result of thermal expansion differences between phases.
3. Surface layers with microcracks formed by a phase transformation.
4. Vitreous or semi-vitreous surface layers.
5. Other surface layers.

Magnesium dititanate bars were cut to form thin plates which were cemented on hot pressed silicon nitride specimens. The room temperature impact resistance of these specimens was substantially improved compared with the impact resistance of controls without the cemented layers. The surface layers crushed under the impacts resulting in the improved impact resistance. Several attempts were made to form magnesium dititanate surface layers on silicon nitride and silicon carbide by hot pressing. These experiments were unsuccessful, primarily due to poor adhesion.

Ceramic bodies consisting of coarse grained silicon carbide in a matrix of fine grained silicon nitride form microcracks in the silicon carbide as a result of the greater thermal contraction of the silicon carbide during cooling after the body is formed at high temperatures. Similar silicon nitride-silicon carbide bodies were formed by hot pressing on hot pressed silicon carbide specimens. Substantial improvements in room temperature impact resistance were observed. The existence of the microcracks in these particular silicon nitride-silicon carbide surface layers was not determined.

Partially stabilized zirconia ceramics can be prepared which contain microcracks resulting from a phase transformation. Thin plates, cut from this material, were cemented to hot pressed silicon nitride specimens and the room temperature impact resistance was measured. No significant improvement in impact resistance was observed. These surface layers fractured instead of crushing, so that less energy was absorbed on impact than in the case of the magnesium dititanate surface layers.

A wide variety of silicate materials were used to form vitreous or semi-vitreous surface layers on silicon carbide and silicon nitride. Petalite ($LiAlSi_4O_{10}$) surface layers on these materials resulted in substantial improvement in impact resistance at elevated temperature. This improvement is attributed to viscous flow of the surface layer material on impact. An improvement in room temperature impact resistance was demonstrated using surface layers of a lead borosilicate frit. Various difficulties, including poor adherence, failure to mature at reasonable temperatures and bubbling, prevented evaluation of specimens with many other treatments.

II. INTRODUCTION

Brittle materials, including silicon carbide and silicon nitride ceramics, are being considered for use as stator vanes in aircraft and stationary gas turbines and rotating parts in automotive gas turbines. A principal difficulty with the proposed use of these materials is their relatively low impact resistance(1). Several approaches are currently being investigated to improve impact resistance, including (a) improvement of the body itself through methods such as fiber reinforcement(2); (b) surface treatments to form compressive surface layers which raise the nominal stress at which surface flaws act to cause failure (3); and (c) surface treatments to form energy absorbing surface layers. It is hoped that the use of one of these strengthening methods or some combination of them will yield sufficient improvement in impact resistance. This report describes an investigation of the third of these approaches, namely, surface treatments to form energy absorbing surface layers.

It is well known that certain materials have outstanding impact resistance. The properties of these materials provide clues that can be used as sources of ideas for improving impact resistance. For example, commercial graphites, if well supported, can be struck a very hard blow without causing more than superficial damage. It is obvious that these materials resist crack propagation in a way that is very different from the easy crack propagation usually observed in polycrystalline ceramics. Of course, commercial graphites lack sufficient oxidation and erosion resistance to be used on the surface of silicon carbide or silicon nitride in gas turbines, but the good impact resistance does lead one to inquire into the specific characteristics responsible for the impact resistance of graphite and to seek these characteristics in other materials.

In this investigation, it has been assumed that the impact resistance of graphite is the result of either microcracks formed due to expansion anisotropy(4), or the easy basal slip, or a combination of these properties. Formation of localized microcracks is a rather common occurrence in polycrystalline ceramics in which it may occur because of thermal expansion anisotropy of individual grains, differences in thermal expansion coefficients between the phases in multi-phase bodies, or changes in volume during phase transformations.

Formation of microcracks due to expansion anisotropy occurs in aluminum titanate(5-7), magnesium dititanate (8, 9), iron titanate(10), titania (rutile)(11,12), V_2O_5(13), Nb_2O_5(14), coarse grained alumina(15,16), beryllia, β-spodumene(17), β-eucryptite(18), boron nitride and other ceramics. This crack formation is responsible for thermal expansion and strength hysteresis. It is also responsible for the very low elastic modulus values observed in these materials(9). The tendency toward microcrack formation increases with increasing grain size. Therefore, it is possible to prepare very strong, high modulus bodies composed of these anisotropic crystals as long as the crystal sizes are small. This is the reason for the success of lithium aluminum silicate glass ceramics. Also, it explains the high strength and elastic modulus of fine grained, hot pressed magnesium dititanate, in which specimens with grains less than 3μm exhibited none of the microcracking attributed to thermal expansion anisotropy(9). Thus, there exists a very wide range of ceramic materials in which microcracks form due to expansion anisotropy.

Microcracks also form as a result of thermal expansion differences between phases in polyphase bodies. R. C. Rossi has investigated several different combinations of phases, especially to obtain low values of elastic modulus and improved thermal shock resistance. Among the systems investigated were "composites" of various carbides with graphite(19), BeO with boron nitride(19), MgO with tungsten(19), and BeO with silicon carbide(20). In a system very closely related to those of interest in this program, Lange(21) observed localized cracks in large grained silicon carbide in a matrix of fine grained silicon nitride.

Another mechanism of localized crack formation involves changes in volume of crystals as a result of phase transformations. It has long been known that large quartz grains break loose from their surroundings in porcelains and refractories when the material cools through the high-low quartz transformation. A more

relevant case is microcrack formation in partially stabilized zirconia. Garvie and Nicholson(22) demonstrated the existence of these microcracks as a result of the cubic-monoclinic phase transformation. Green, Nicholson and Embury(23) state that the formation of the microcracks results in a material of very low elastic modulus (10,300 MNm^{-2}). Microcracked zirconia may be a promising material for energy absorbing surface layers because of its refractoriness and low elastic modulus.

Another, somewhat different, means of energy absorption that might be used to absorb impact is viscous flow. Rhodes and Cannon(2) achieved a substantial increase in impact resistance at high temperatures as a result of using a thin lithium aluminum silicate (β-spodumene composition) surface layer which might be expected to deform by viscous flow at elevated temperatures. Viscous shear, compressive surface layers and elimination of surface flaws were discussed as possible explanations of this improvement. It may be significant that a similar improvement in impact resistance was not observed at room temperature.

In the present investigation, surface treatments were used to form the following types of energy absorbing surfaces on hot pressed silicon nitride and silicon carbide:

1. low elastic modulus surface layers with microcracks caused by thermal expansion anisotropy.

2. low elastic modulus surface layers with microcracks caused by thermal expansion differences between phases.

3. low elastic modulus surface layers with microcracks caused by volume changes during phase transformations.

4. low elastic modulus, vitreous or semi-vitreous surface layers that absorb energy by viscous flow.

Some of the materials chosen for investigation in this program can be expected, with further development, to have properties useful for practical applications. Other materials are unlikely to be useful for practical applications but were chosen, as model materials, to demonstrate the advantages of particular mechanisms.

The impact resistance of the treated specimens was measured at room temperature and at elevated temperatures. The treated specimens and the fracture surfaces of the impact

tested specimens were characterized. Substantial improvements in impact resistance through the use of energy absorbing surface layers were achieved.

The procedures by which these improvements were achieved are described in the next section. Following that, the results are presented and discussed.

III. PROCEDURES

A. Materials

Billets of hot pressed silicon nitride* (6 x 6 x 1.1 in.) and silicon carbide** (9 in. diameter x 1.1 in.) were purchased. The specific gravities of the materials as determined by the manufacturer for the particular billets were 3.18 for the silicon nitride and 3.35 to 3.37 for the silicon carbide.

Before the materials ordered especially for this program were delivered, preliminary experiments were conducted using already available materials, including Norton hot pressed silicon nitride and silicon carbide, AVCO hot pressed silicon nitride, and Alfred Ceramic Enterprises silicon carbide.

The Norton silicon nitride and silicon carbide intended for use in the principal experiments in this investigation were characterized by electron microscopy and scanning electron microscopy. An electron micrograph of a polished and etched specimen of silicon nitride is presented in Figure 1. This specimen was mounted in plastic, polished with 6 μm diamond paste on a tin platen, using moderate to heavy pressure and etched in a 50-50 weight percent solution of KOH and NaOH at 300°C. The specimen is overetched, but the elongated one to three micrometer grains that make up the body are evident.

Photomicrographs of Norton silicon carbide are presented in Figure 2. The upper picture is a scanning electron micrograph of a fracture surface. This picture shows that the typical grains are three to ten micrometers in size. The fracture is predominantly intergranular. The lower picture is an electron micrograph of the fracture surface and shows the grains and grain boundaries at somewhat higher magnification.

---

* NORALIDE NC-132, Norton Company, Worcester, Mass.

** NORALIDE NC-203, Norton Company, Worcester, Mass.

Figure 1 - Microstructure of Hot Pressed Norton NC-132 Silicon Nitride (12,500X, Specimen GB-23-14)

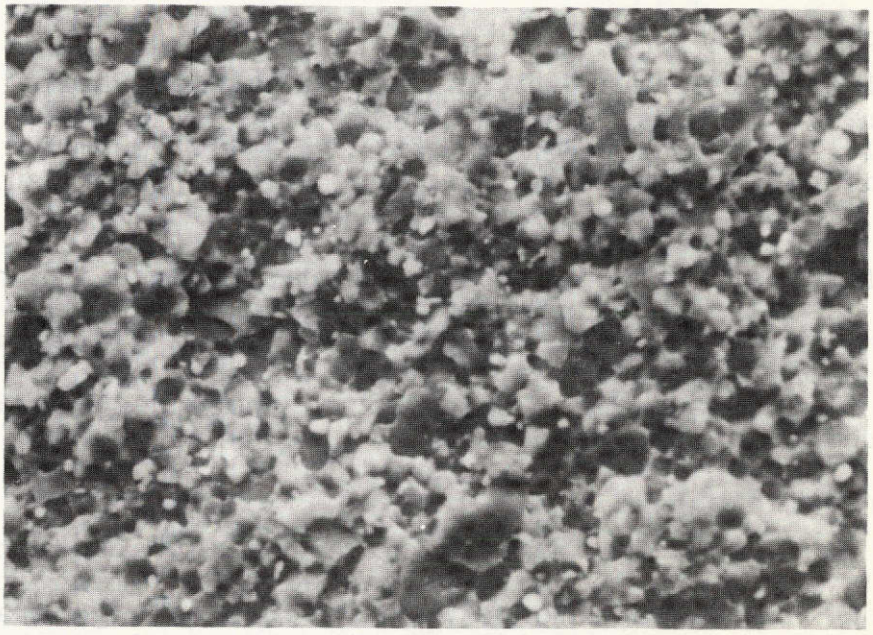

A. 1000X

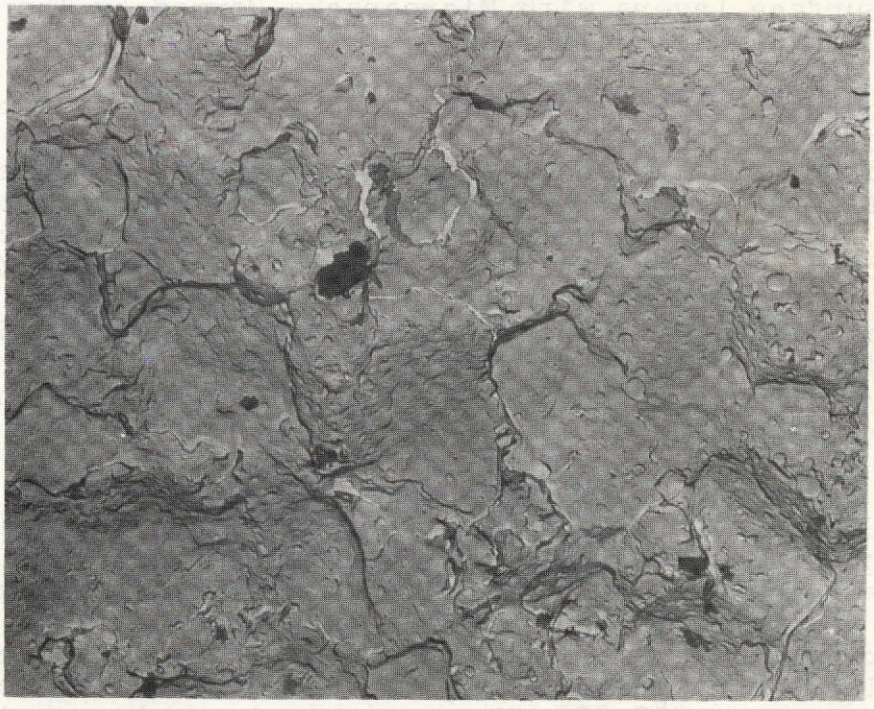

B. 6035X

Figure 2 - Microstructure of Hot Pressed Norton NC-203 Silicon Carbide (Specimen JS-52-212, Billet no. 435556)

This page is reproduced at the back of the report by a different reproduction method to provide better detail.

B. Specimen Fabrication

The billets were cut to form unnotched Charpy test specimens 6.4 x 6.4 x 57 mm (0.25 x 0.25 x 2.25 in.) and 10 x 10 x 57.2 mm (0.4 x 0.4 x 2.25 in.). In many cases, the edges of these specimens were rounded on a diamond lap using diamond paste.

In some cases, flat plates were prepared for treatment. Usually the dimensions of these plates were 63.5 x 32 x 6.3 mm (2.5 x 1.1 x 0.25 in.). These plates were treated on the two large surfaces and then cut to form Charpy impact specimens, similar to those described above, but treated on two surfaces.

C. Treatments

Specimens were treated to form energy absorbing surface layers using the methods listed in the main introduction. These treatments were described in general in this section. The specific treatments are described, together with the results of the particular experiments, in Section IV.

1. Surface Layers with Microcracks Formed by Thermal Expansion Anisotropy

Some of the polycrystalline ceramics forming microcracks as a result of thermal expansion anisotropy were listed previously, and a substantial number of other such materials are known. The secondary characteristics of these materials were reviewed in an effort to select the most promising materials for surface treatments. Most of these materials are unsuitable because of chemical or thermal instability and others, such as alumina and beryllia seem likely to form microcracks only after extreme grain growth has occurred. As a result of this review, magnesium dititanate and aluminum titanate were selected as the most promising materials.

Specimens of magnesium dititanate with a variety of average grain sizes were provided by Professor R. C. Bradt of The Pennsylvania State University. These specimens are those described in the recently published paper of Kuszyk and Bradt(9). The tendency to form microcracks increases with increasing grain size. Therefore, the elastic modulus decreases from 240,000 MNm^{-2} at one micrometer grain size to 55,000 MNm^{-2} at seven micrometer grain size and 31,000 MNm^{-2} at 48 μm grain size.

In preliminary experiments to evaluate the magnesium dititanate as an energy absorbing material, thin plates were cut from 5μm and 15μm specimens supplied by Professor Bradt. These thin plates were cemented* to the surface of Charpy impact test bars. Only the portion of the specimen at and near the impact point was covered by the cemented plate. The portions of the specimen in contact with the specimen supports were not covered. Presumably, this arrangement should lead to a conservative result because of the enhanced rigidity at the supports.

Preparation of magnesium dititanate powder

In order to provide our own source of powder for additional experiments, magnesium dititanate was prepared, using TiO_2** and $MgCO_3$***. Heating the $MgCO_3$ at 1100°C in air for one hour yielded a residue 43% the weight of the original powder. In calculating the proportions of the reactants, this residue was assumed to be entirely MgO. The resulting batch was 37% $MgCO_3$ and 63% TiO_2, with a total weight of 100 grams. The materials were mixed by ball milling in acetone for one-half hour with alumina balls. After drying in an evacuated oven at 90°C, the powder was placed loosely in fire clay crucibles and fired in air at 1300°C for one hour. The once-fired material was ball milled in acetone for two hours. Due to reaction with crucibles, the material was transferred to a new crucible and refired in air at 1300°C for one hour. Then, the material was ground with a mortar and pestle and fired a third time, using the same procedure. After grinding the material again using the mortar and pestle, and passing the material through a 200 mesh sieve, the material was considered ready for use in forming surface layers. X-ray diffraction analysis showed that the material consisted essentially of magnesium dititanate and that there was no evidence of substantial amounts of second phases.

Magnesium dititanate surface layers

The magnesium dititanate powder was used to form surface layers on silicon carbide and silicon nitride by hot pressing in a graphite die. A thin layer of the powder was placed in a graphite die. Then, a plate of

---

* White rubber paper cement, Union Rubber and Asbestos Co.

** Baker analyzed reagent, lot no. 38356.

*** Mallinckrodt analyzed reagent (approximately $4MgCO_3 \cdot Mg(OH)_2 \cdot 4H_2O$).

silicon carbide or silicon nitride in a graphite retainer was placed on the powder. The graphite retainer was designed to prevent the specimen from deforming too much. Then, another layer of magnesium dititanate was placed on the specimen. The remainder of the graphite die was assembled and the specimen was hot pressed at 1100 or 1200°C for one hour at 20.7 MNm^{-2}. In some cases, hot pressed controls (no magnesium dititanate) were processed in the die in the same run in which the treated specimen or specimens were processed.

The treated material was removed from the die and cut to form bars. The impact resistances of the treated specimens were measured and the surface layers were characterized.

The microstructures of the magnesium dititanate material used for the cemented plates were presented by Kuszyk and Brandt(9). A scanning electron micrograph of a fracture surface of similar material hot pressed at Ceramic Finishing Company at 1200°C and 20.7 MNm^{-2} for one hour is illustrated in Figure 3.

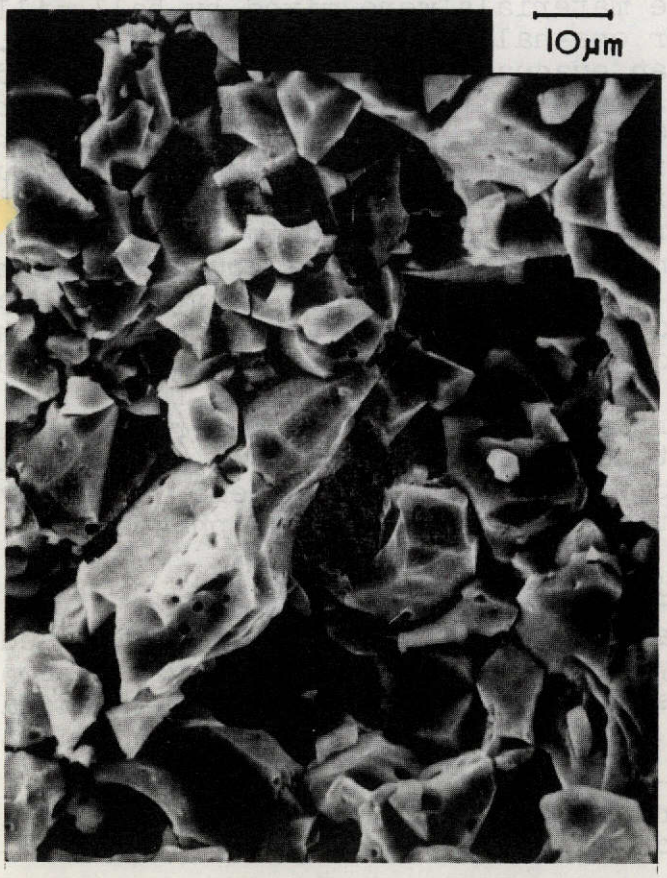

Figure 3 - Fracture Surface of Magnesium Dititanate, as Hot Pressed, Ten Micrometer Average Grain Size (1000X)

The picture shows a multitude of intergranular cracks resulting in a very loosely bonded structure. Also, occasional transgranular cracks are present. Therefore, the reasons for the low strength and low elastic modulus of this material are evident.

Aluminum titanate was selected as the second most promising of these materials. The principal problem with this material is that it tends to decompose when held for long periods of time at temperatures under 1400°C. Since this decomposition temperature corresponds to the proposed use temperature of the silicon carbide and silicon nitride, it is evident that the decomposition of the aluminum titanate must be prevented for this material to become useful. There is evidence that the solution to this problem is known (F. J. Brodman, General Refractories Co.) but the information is not yet available to us. Therefore, experiments using this material have not yet been done.

2. Surface Layers with Microcracks Resulting from Thermal Expansion Differences between Phases

This particular type of energy absorbing surface layer is considered especially promising because the very wide range of possible surface layer compositions increases the opportunities for compatibility of the surface layer and the body, and allows consideration of secondary surface layer characteristics, such as erosion resistance. Surface layer materials consisting of coarse grained silicon carbide in a fine grained matrix of silicon nitride were selected for these experiments. These materials are similar to those described by Lange(21) in which microcracks were observed in the coarse grained silicon carbide. Presumably, these cracks form to relieve tensile stresses induced during cooling after hot pressing, when the silicon carbide tends to contract more than the silicon nitride matrix.

Two types of silicon nitride were used. In the preliminary experiments, an already available material* was used. In later experiments, a more recently developed high alpha silicon nitride powder** was used. Various

---

* Hermann C. Starck, Berlin, silicon nitride lot no. T 3619, analysis Si-56.9%, N-39.6%, C 0.18%, 1.05 μm grain size.

** Advanced Materials Engineering, Ltd., Durham England. silicon nitride, 85% minimum alpha phase, -300 mesh.

percentages (10, 20, and 30%) of 280 or 400 mesh silicon carbide* were mixed with the silicon nitride together with 5% by weight relative to the silicon nitride of MgO (added as $MgCO_3$**) added to aid sintering. It should be pointed out that whereas impurities and sintering aids in the main body are detrimental because they increase the creep rate, they may be advantageous to the surface layer because increased creep rate may increase energy absorption in the surface layer at high temperatures. These powders were mixed by milling with t-butanol in an alumina mill with alumina balls for about one hour and dried at 90°C in a vacuum oven.

The coatings were applied to both silicon carbide and silicon nitride specimens and were formed by both hot pressing and conventional sintering. The hot pressing technique was similar to that described above for magnesium dititanate surface layers. Because of the higher temperatures used in this case, the use of the graphite retainer to reduce the deformation of the bodies was even more essential than in the previous cases. The time, temperature and pressure were varied in efforts to obtain reasonable density in the surface layer while at the same time minimizing any effects on the main body. Graphite foil*** and boron nitride powder**** were used as separators to reduce sticking of the materials to the graphite die. In some cases, it was difficult to remove these materials from the hot pressed specimen, and it was necessary to do this by hand sanding. The good abrasion resistance of the surface layers was evident in some cases during this sanding. The plate with the hot pressed surface layers on two sides was cut to provide Charpy test specimens.

3. Surface Layers with Microcracks Formed as a Result of Volume Changes During Phase Transformations

A piece of partially stabilized zirconia of the type described as containing microcracks by Green, Nicholson and Embury(23) was generously supplied by Professor Nicholson.

---

* Norton Company, Worcester, Mass., crystolon silicon carbide.

** Fisher certified $MgCO_3$.

*** Union Carbide Co., New York, Grafoil Grade GTB.

**** Cerac, Inc., Menomonee Falls, Wisconsin boron nitride SP-107.

Thin plates cut from this material were cemented on the impact area of silicon nitride impact bars in the same manner as described for magnesium dititanate. The impact resistance of these specimens was measured.

4. Vitreous or Semi-Vitreous Surface Layers

As mentioned previously, experiments reported by Rhodes and Cannon(2) in which β-spodumene ($LiAlSi_2O_6$) composition surface layers, 10 μm thick, were formed on silicon nitride, resulted in a substantial improvement in impact resistance at high temperatures. After firing, the surface layers consisted of at least two phases, one amorphous and one crystalline. At least part of the improvement in impact resistance was attributed to viscous shear.

Based upon these favorable results, a wide range of vitreous or semi-vitreous surface layers were formed on silicon carbide or silicon nitride specimens. Each surface layer material posed a somewhat different set of problems so the processes used to form each coating will be described separately.

Spodumene ($LiAlSi_2O_6$)

The choice at AVCO of spodumene to form surface layers on silicon nitride may have been based upon the knowledge that glasses near this composition have low thermal expansion coefficients. It is, perhaps, a coincidence that the lithium aluminum silicate crystalline phases are highly anisotropic so that the possibility of formation of microcracks must be kept in mind. However, until evidence of this is available, these treatments will be classified as vitreous or semi-vitreous surface layers in which energy is absorbed by viscous flow.

Spodumene, in the form of a natural ground mineral*, was used in these experiments. The powder was mixed with water to form a slip which was applied to the silicon nitride or silicon carbide by dipping, spraying or painting. The specimens were fired at temperatures ranging from 1275° to 1450°C for various periods of time. On silicon nitride, the most successful firing temperature range was 1375° to 1425°C, and a reducing atmosphere was necessary. No successful temperature range was found for treating silicon carbide.

* Ceramic Color and Chemical Mfg. Co., New Brighton, Pa.

Petalite ($LiAlSi_4O_{10}$)

Petalite is another lithium aluminum silicate phase that can melt to form low expansion glasses. Again, the material was used in the form of a ground mineral powder* which was applied to the specimens as described for spodumene. The best temperature was 1400°C and reducing conditions were necessary.

G-24 frit

Frits are partly or completely fused compounds that are used as a basis for certain glazes. The G-24 frit is a lead borosilicate frit and has the following composition: SiO_2, 53.5%; Al_2O_3, 8.42%; B_2O_3, 7.44%; ZrO_2, 1.33%; Na_2O, 2.24%; CaO, 6.53%; MgO, 0.80%; PbO, 18.30%; K_2O, 1.41%; and Fe_2O_3, 0.04%. It was applied as described previously for the other materials.

D. Impact Testing

The principal property measurement used in this investigation was impact resistance. A Bell Telephone Laboratories type Charpy impact testing machine** was used. This machine was modified by placing an induction heated furnace and specimen support between the pendulum supports, to enable testing from room temperature to 1400°C. The specimen support span was 3.8 cm (1.5 in.)

Impact testing of brittle materials has been the subject of recent investigations by Davidge and Phillips(24) and Leuth(25). It is clear from these investigations that there are substantial problems in applying impact testing to brittle materials. These problems arise because the impact resistance is quite low, so that the various errors in testing are more significant than is the case in testing more impact resistant materials.

E. Characterization

The silicon nitride and silicon carbide bodies used in this investigation were studied by optical and electron microscopy as described previously. The surface layers were also studied by optical microscopy. The composition and constitution of the surface layers were determined in some cases

* Ceramic Color and Chemical Mfg. Co., New Brighton, Pa.

** Satec Systems, Inc., Grove City, Pa.

by electron probe microanalysis and by x-ray diffraction analysis. The thickness and density (porosity) of the surface layers were measured.

The fracture surfaces of most of the specimens were studied by optical microscopy. A simple, consistent method of examination was used in an effort to provide information suitable for later interpretation. The location of the fracture was noted. If it was judged to have occurred at the center of the span that fact was noted, using the comment "break in center". If it was judged to have occurred near the center of the span, but noticeably off center, it was noted as "break near center". If fractures also occurred at one or both ends, that was noted, also.

The position of the fracture origin on the fracture surface was described using the following terms:

(1) origin at corner - meaning the origin of the fracture was located at an edge of the original bar, thus at a corner of the fracture surface.

(2) origin at edge - meaning the origin of the fracture was located in one face of the original bar, thus, at an edge of the fracture surface.

(3) origin __ μm from edge - meaning that the origin of the fracture was located in the interior rather than on the surface and at the stated distance from the surface.

The quality of the fracture mirror was evaluated. This was, perhaps, the most difficult item on which to maintain consistency and objectivity. In each case, the quality of the mirror was rated good, fair or poor, and the mirror radius (radius at crack branching) was estimated. The reliability of the mirror radius measurements improved substantially with increasing quality of the fracture mirror. In many cases, the mirror measurements of the poorer mirrors were not recorded because of lack of reliability. The mirror radius measurements were used in some cases to estimate the fracture stresses at which the impact fractures occurred. This was done using fracture stress vs. mirror size curves (26).

IV. RESULTS AND DISCUSSION

A. Impact Resistance of Control Specimens

In this section, the impact resistances of the various types of control specimens are collected and compared. Measurements are reported for both standard and large size specimens of Norton silicon carbide. Some of the materials were tested at room temperature and at elevated temperatures.

1. Norton NC-132 Silicon Nitride

The impact resistances of standard test bars of Norton NC-132 silicon nitride were measured at room temperature. These specimens were cut from the billet obtained especially for this program. The results are given in Table I, and show that, within the limits imposed by the variability of the impact testing, the impact resistance of this material is the same as that observed for the other billets of hot pressed Norton silicon nitride tested earlier.

The fracture mirrors formed in Norton NC-132 silicon nitride fractured in impact are more well defined than those formed in silicon carbide under similar conditions. The small size of the fracture mirrors indicates that these fractures occurred at high stresses. These fracture stresses are in the range expected if similar specimens were tested in ordinary flexure tests.

The impact resistance of Norton silicon nitride control specimens cut from other billets used for preliminary experiments are collected in Table II. Due to the small number of specimens in each group, it is unlikely that the results reported in this table are significantly different from the results reported in the previous table.

2. AVCO Silicon Nitride

The impact resistances of AVCO silicon nitride control specimens are given in Table III. The results obtained for three small groups of specimens were essentially equivalent with averages ranging from 0.32 to 0.35 Joules. The elevated temperature measurements (1325°C) averaged 0.55 Joules. This higher value may be significantly different from the room temperature values.

The fracture surfaces of the specimens tested at room temperature were somewhat unique in that the fractures originated at a variety of places, rather than at one particular type of location. Fractures originated at corners, edges and internally.

TABLE I

IMPACT RESISTANCE OF NORTON NC-132 SILICON NITRIDE

(As machined, nominal dimensions 6.3 x 6.3 x 57.2 mm)

Billet No. SN-10-12-72A

Specimen No.	Room Temperature Impact Resistance (1) Joules	in.lbs.	Mirror Radius μm	Comments
JS-48-1	0.28	2.5	250	Break near center, origin at corner, good mirror
JS-48-2	0.54	4.8	--	Unusual break, origin may be at edge on impact side
JS-48-3	0.31	2.7	100	Break near center, origin 50 μm from edge, good mirror
Average	0.37	3.3		

(1) one foot pound hammer

TABLE II - IMPACT RESISTANCE OF NORTON SILICON NITRIDE CONTROL SPECIMENS

Specimen No.	Type	Size	Test Temp. °C	Impact Resistance[1] Joules	in. lbs.	Mirror Radius µm	Comments
JSP-1-C1	Norton HS-130	Standard	25	0.60	5.3	200	Break in center, origin at corner, good mirror
-2-C1	"	"	"	0.32	2.8	125	Break in center, origin near corner, good mirror
			Average	0.46	4.1		
JSP-15-C1	Norton HS-130	Standard	25	0.28	2.5	175,175	Break in center, origins at two corners, good mirrors
-C2	"	"	"	0.33	2.9	150	Break in center, origin at corner, very good mirror
			Average	0.31	2.7		
JSP-24-C1	Norton HS-130	Standard	25	0.40	3.5	200	Break in center, origin at corner, poor mirror
-C2	"	"	"	0.29	2.6	200	Break in center, origin at corner, good mirror, weak looking fracture
			Average	0.35	3.1		
G-29-11[2]	Norton NC-132, rounded edge	Standard	25	0.32	2.8	---	
-12	"	"	"	0.27	2.4	---	
-13	"	"	"	0.44	3.9	---	
G-35-9	"	"	"	0.44	3.9	---	
-10	"	"	"	0.35	3.1	---	
-11	"	"	"	0.40	3.5	---	
G-33-9	"	"	"	0.31	2.7	---	
-10	"	"	"	0.34	3.0	---	
-11	"	"	"	0.33	2.9	---	
			Average	0.35	3.1		

(1) one foot pound hammer (2) results from Contract No. NAS3-16788

TABLE III - IMPACT RESISTANCE OF AVCO SILICON NITRIDE CONTROL SPECIMENS

Specimen No.	Type	Size	Test Temp. °C	Impact Resistance(1) Joules	in.lbs.	Mirror Radius µm	Comments
JS-34-C1	As machined	Standard	25	0.42	3.8	100	Break at center, origin 50 µm from edge, fair mirror
-C2	"	"	"	0.26	2.3	250	Break at center, origin at edge, good mirror
-C3	"	"	"	0.34	3.0	---	Break at center, origin at corner, poor mirror
		Average		0.34	3.0		
JSP-23-C1	As machined	Standard	25	0.27	2.4	125	Break at center, origin 50 µm from edge, good mirror
-C2	"	"	"	0.36	3.2	---	Break near center, origin uncertain
		Average		0.32	2.8		
JS-31-A	As machined	Standard	25	0.32	2.8	---	Break at center, origin at corner, poor mirror
-B	"	"	"	0.25	2.2		Break at center, origin at or near corner, poor mirror
-C	"	"	"	0.48	4.3	125	Break at center, origin 50 µm from edge, good mirror
		Average		0.35	3.1		
JS-31-AET	As machined	Standard	1325	0.67	5.6	100	Break at center, origin 175 µm from corner, good mirror
-BET	"	"	"	0.52	4.6	---	Break near center, origin at corner, poor mirror
-CET	"	"	"	0.45	4.0	---	Break at center, origin at corner, poor mirror
		Average		0.55	4.7		

(1) one foot pound hammer

3. Norton NC-203 Silicon Carbide

Impact tests were run at room temperature and three elevated temperatures using specimens cut from the billets obtained for this investigation. These results are presented in Table IV. The results show that there is a small increase in impact resistance with increasing temperature.

The fractures in Norton NC-203 silicon carbide at room temperature tend to occur at or near the center of the span, originate at corners, and form poor fracture mirrors. At 1100° and 1200°C, there is an increased tendency for fractures to occur both at the center and at one end. Because of the poor quality of the fracture mirrors, the estimates of mirror radius are crude. There is no reliable indication of variation in mirror size with temperature.

In the case of the two incorrect measurements not included in the averages, the fracture surfaces appear similar, in most respects, to those of the other specimens. Therefore, it seems likely that, if these measurements had been made correctly, the impact resistances would have been in the normal range and the averages would not be changed significantly.

The results of other earlier measurements of Norton NC-203 control specimens are given in Table V. The results for the standard size specimens tested at room temperature and at 1325°C are similar to those reported in the previous table.

Larger specimens (10.2 x 10.2 mm. in cross section) were tested. Because of the design of the test fixtures, the space available for the fractured specimen to fall past the hammer is quite small. With the large specimens, there seems to be substantial risk of jamming. Therefore, only one group of large specimens was measured. The average impact resistance of these specimens was 1.08 Joules.

One can assume that failure of the silicon carbide bars occurs when the outer fiber stress of the point on the opposite surface to the impact surface reaches the maximum strength of silicon carbide. From beam theory, one would expect about 2.5 times the work would be required to deflect the large bar to reach this stress than it would take to deflect the small bar to the same stress. The measured ratio of the impact resistances is 4.8, a value much different from the ratio calculated on the basis of this assumption. Dinsdale et al(27) analysed the impact response of ceramics in terms of elastic deflection

TABLE IV - IMPACT RESISTANCE OF NORTON NC-203 SILICON CARBIDE AT VARIOUS TEMPERATURES
(Nominal Dimensions 6.3 x 6.3 x 57.2 mm)

Specimen No.	Test Temp. °C	Impact Resistance[1] Joules	in.lbs.	Mirror Radius µm	Comments
Billet No. 433646					
JS-52-ART	25	0.21	1.9	375	Break near center, origin at corner, fair mirror
-BRT	"	-- [2]	--	--	Break at center, origin at corner, poor mirror
-CRT	"	0.21	1.9	375	Break near center, origin at corner, fair mirror
Average		0.21[4]	1.9		
JS-52-11A	1100	0.42	3.7	250	Break at center, origin at corner, poor mirror
-11B	"	0.37	3.3	250	Break at center, origin at corner, poor mirror
-11C	"	0.33	2.9	--	Break at center and one end, origin at corner, large mirror
Average		0.37	3.3		
JS-52-12A	1200	0.49	4.3	375	Break at center and one end, origin at corner, poor mirror
-12B	"	--	11.0[3]	--	Break near center, origin at corner near inclusion, large mirror
-12C	"	0.47	4.2	375	Break at center, origin at corner, poor mirror
Average		0.48[4]	4.3		
JS-52-13A	1325	0.36	3.2	375	Break at center, origin at corner, poor mirror
-13B	"	0.44	3.9	375	Break near center, origin at corner, poor mirror
-13C	"	0.62	5.5	--	Break at center, origin at corner, poor mirror
Average		0.47	4.2		

TABLE IV - (continued)

Specimen No.	Test Temp. °C	Impact Resistance(1) Joules	Impact Resistance(1) in.lbs.	Mirror Radius µm	Comments
Billet No. 435556					
JS-52-1RT	25	0.09	0.8	375	Break at center, origin at corner, good mirror
-2RT	"	0.23	2.0	375	Break at center, 6 pieces, origin at corner, fair mirror
-3RT	"	0.21	1.9	250	Break near center, origin at corner, poor mirror
Average		0.18	1.6		
JS-52-111	1100	0.26	2.3	375	Break at center and one end, origin at corner, poor mirror
-211	"	0.24	2.1	--	Break near center, origin at corner, poor mirror
-311	"	0.34	3.0	375	Break at center and one end, origin at corner, good mirror
Average		0.28	2.5		
JS-52-112	1200	0.78	6.9	250	Break near center, origin at corner, poor mirror
-212	"	0.66	5.8	--	Half of specimen missing
-312	"	0.33	2.9	375	Break near center, origin at corner, poor mirror
Average		0.59	5.2		
JS-52-113	1325	0.42	3.7	--	Break near center, origin at corner, poor mirror
-213	"	0.32	2.8	--	Break at center, origin at corner, large mirror
-313	"	0.26	2.3	250	Break at center, origin at corner, good mirror
Average		0.33	2.9		

(1) one foot pound hammer

(2) no result, forgot to reset pointer

(3) specimen jammed

(4) average of two values

TABLE V - IMPACT RESISTANCE OF NORTON NC-203 SILICON CARBIDE CONTROL SPECIMENS

Specimen No.	Type	Size	Test Temp. °C	Impact Resistance[1] Joules	Impact Resistance[1] in.lbs.	Mirror Radius μm	Comments
JS-31-1	As machined	Standard[2]	25	0.21	1.9	250	Break at center, origin at corner, poor mirror
-2	"	"	"	0.20	1.8	250	Break at center, origin at corner, good mirror
-3	"	"	"	0.26	2.3	200	Break at center, origin at corner, good mirror
			Average	0.22	2.0		
JS-31-1ET	As machined	Standard	1325	0.25	2.2	--	Break at center and one end origin uncertain
-2ET	"	"	"	0.72	6.4	--	Break at center, origin at corner, large mirror
-3ET	"	"	"	0.50	4.4	--	Break at center, weak looking fracture
			Average	0.49	4.3		
JS-40-1	As machined	Standard	25	0.23	2.1	250	Break at center, origin at corner, fair mirror
-2	"	"	"	0.20	1.7	250	Break near center, origin at corner, poor mirror
-3	"	"	"	0.25	2.2	--	Break near center and one end, origin at corner
			Average	0.22	2.0		
JS-40-4	As machined	Large[3]	25	1.16	10.3[4]	--	Break at one one, origin uncertain
-5	"	"	"	0.99	8.8[4]	200	Break at center, origin at corner, fair mirror
-6	"	"	"	--	--[4,5]	--	Break at two ends, origin uncertain, many flakes
			Average	1.08	9.6		

(1) one foot pound hammer unless otherwise noted
(2) Standard specimen dimensions nominally 6.35 x 6.35 x 57 mm
(3) Large specimen dimensions nominally 10.2 x 10.2 x 57 mm
(4) two foot pound hammer
(5) the specimen broke at the supports, leaving a piece which straddled the support and stopped the hammer from swinging through

energy, indentation energy and shear energy. In an extensive investigation of the impact resistance of silicon carbide, Ashford and Priddle(28) investigated two criteria for impact fracture (1) stored energy and (2) Hertzian contact stresses. Also, the energy losses caused by transfer of energy to the testing machine may vary with the impact resistance of the machine. In view of all of these possibilities, it is not surprising that the measured impact resistance did not increase in proportion to the cross sectional area.

B. Surfaces with Microcracks Caused by Thermal Expansion Anisotropy

1. Magnesium Dititanate on Silicon Nitride

Thin plates of magnesium dititanate with 5 and 15 μm grain size were cemented on Norton HS-130 silicon nitride bars at the impact point. The impact resistances of the specimens were measured and are presented in Table VI. In tests at room temperature using a one foot pound hammer, none of the treated specimens fractured under the impact. These results indicate at least a three-fold improvement in impact resistance as a result of the low elastic modulus surface with microcracks caused by expansion anisotropy. One of these specimens is illustrated in Figure 4. This figure shows the crushing that occurred when the hammer struck the specimen.

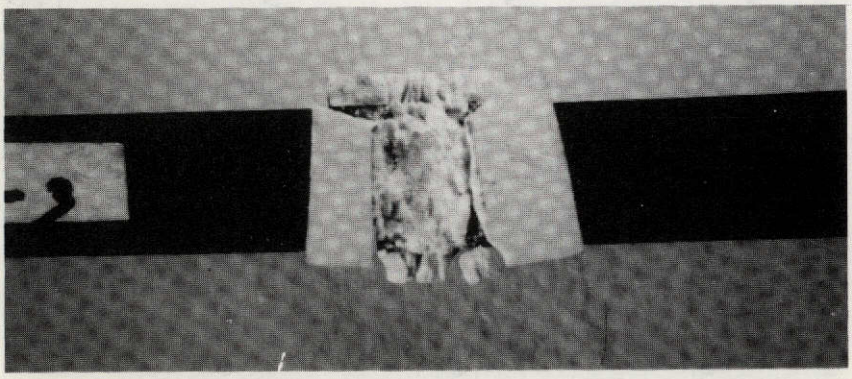

Figure 4 - Impact Test Specimen with Cemented Magnesium Dititanate Plate (3X)

TABLE VI

IMPACT RESISTANCE OF NORTON HS-130 SILICON NITRIDE BARS WITH CEMENTED PLATES OF MAGNESIUM DITITANATE

(6.4 x 6.4 x 57 mm bars)

Specimen No.	Treatment	Layer Thickness mm	Room Temp. Impact Resistance (1) Joules	in.lbs.
JSP-1-C1	Control	none	0.60	5.3
-2-C1	"	"	0.32	2.8
		Average	0.46	4.1
JSP-1-1	15 μm $MgTi_2O_5$	0.97	>1.36	>12
-2	"	1.21	>1.36	>12
-3	"	1.35	>1.36	>12
		Average	>1.36	>12
JSP-2-1	5 μm $MgTi_2O_5$	0.73	>1.36	>12
-2	"	0.75	>1.36	>12
-3	"	0.77	>1.36	>12
		Average	>1.36	>12

(1) one foot pound hammer

These experiments were continued by cementing magnesium dititanate plates of the two different grain sizes and varying thicknesses to AVCO silicon nitride bars. The impact resistances of these specimens were measured at room temperature using the two foot pound hammer to assure that the specimens fractured. The results are presented in Table VII. The impact resistances of the specimens with cemented magnesium dititanate plates were substantially higher than the controls, and the improvement increased with increasing thickness of the plates. No definite effect of grain size was observed.

Because of the above promising results, efforts were made to form magnesium dititanate surfaces by directly bonding the material to the surface of the silicon nitride or silicon carbide. The method chosen was hot pressing. These experiments failed because of poor adherence. The results are summarized briefly in the following paragraphs.

Magnesium dititanate powder was spread in a thin layer above and below a slab of AVCO silicon nitride in a hot pressing die. Another slab, for hot pressed control specimens, was placed in the die. Both slabs were placed in graphite retainers to limit the deformation. The materials were pressed at 1100°C and 20.7 MNm^{-2} for one hour. The magnesium dititanate layers adhered poorly and on one side of the slab came off in large flakes. The hot pressed slab in the graphite retainer is illustrated in Figure 5. The silicon nitride slab is outlined by the white line. The magnesium dititanate did not adhere to the graphite retainer and is shown coming off in large flakes. The lack of adhesion of the magnesium dititanate to the silicon nitride is less obvious, but is indicated by the cracks that cross the white line into the area of the silicon nitride slab.

Bars were cut from the slabs and the impact resistances were measured. The side to which the magnesium dititanate adhered best was placed on the impact side. The surface layer shattered on impact, rather than crushing, and no improvement in impact resistance was observed (see Table VIII).

The fractures of the hot pressed controls were similar to the as machined AVCO controls. The specimens fractured in the center of the span and the fractures had a strong tendency to originate at or near corners. When mirrors were observable, they were relatively small.

The fractures of the specimens with $MgTi_2O_5$ surface layers were similar to the hot pressed controls and the as machined controls. The most interesting observation was obtained using specimen GB-13-2, which even though it formed a good mirror, did not appear to show crack branching.

TABLE VII

IMPACT RESISTANCE OF AVCO SILICON NITRIDE BARS WITH CEMENTED PLATES OF MAGNESIUM DITITANATE

(6.4 x 6.4 x 57 mm bars)

Specimen No.	Treatment	Layer Thickness mm	Room Temp. Impact Resistance(1) Joules	in.lbs.
JS-34-C1	Control	---	0.42	3.8
-C2	"	---	0.26	2.3
-C3	"	---	0.34	3.0
	Average	---	0.34	3.0
JS-34-5A	5 µm $MgTi_2O_5$	1.25	1.07	9.5
-5B	"	1.31	1.15	10.2
-5C	"	1.34	2.38	21.1
	Average	1.30	1.53	13.6
JS-34-5D	5 µm $MgTi_2O_5$	0.54	0.46	4.1
-5E	"	0.58	0.47	4.2
-5F	"	0.63	0.41	3.6
	Average	0.58	0.45	4.0
JS-34-15A	15 µm $MgTi_2O_5$	1.12	1.24	11.0
-15B	"	1.07	1.28	11.3
-15C	"	0.91	1.24	11.0
	Average	1.03	1.25	11.1
JS-34-15D	15 µm $MgTi_2O_5$	0.26	0.35	3.1
-15E	"	0.31	0.43	3.8
-15F	"	0.44	0.64	5.7
	Average	0.34	0.47	4.2

(1) two foot pound hammer

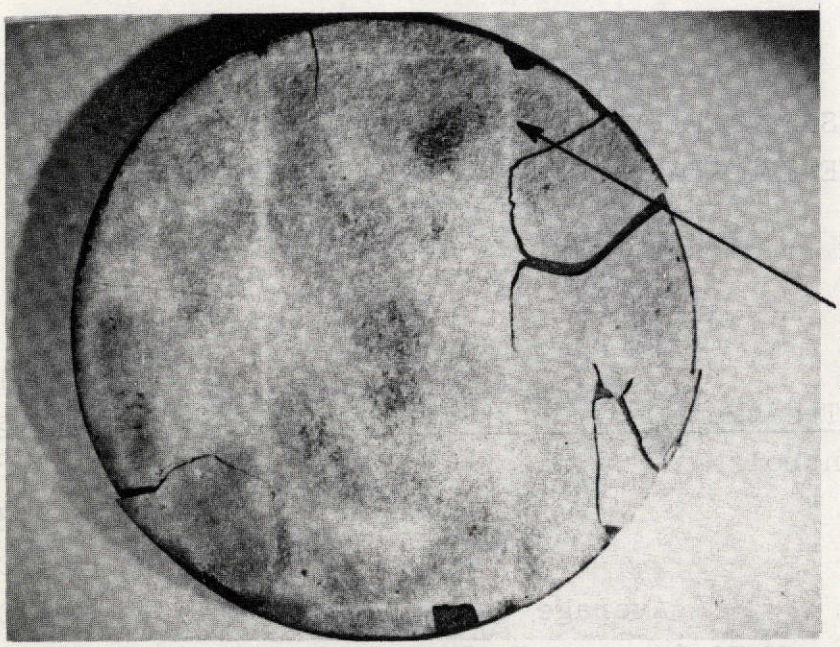

Figure 5 - Hot pressed Magnesium Dititanate on AVCO Silicon Nitride

In a further attempt to form a magnesium dititanate surface on AVCO silicon nitride, slabs were pressed at 1200°C and 20.7 MNm^{-2} for one hour, using a similar arrangement. The higher temperature was chosen in the hope that it would result in improved adhesion, but this was not observed.

Even though the slabs did not retain the surface layers, they did show surface discoloration, indicating that some reaction may have occurred. Therefore, bars were cut and tested at room temperature. A small increase in impact resistance was observed for the treated material, compared with the hot pressed controls, but neither of these groups was better than as machined controls.

TABLE VIII

IMPACT RESISTANCE OF AVCO SILICON NITRIDE WITH HOT PRESSED $MgTi_2O_5$ SURFACE LAYERS

Specimen No.	Treatment	Layer Thickness mm	Room Temp. Impact Resistance[1] Joules	in.lbs.	Mirror Radius μm	Comments
GB-13-4C	Hot pressed control	--	0.36	3.2	150	Break at center, origin near corner, fair mirror
-5C	"	--	0.31	2.8	--	Break at center, origin at corner, poor mirror
-6C	"	--	0.37	3.3	100	Break at center, origin near corner, fair mirror
	Average	--	0.35	3.1		
GB-13-1	Hot pressed $MgTi_2O_5$	0.71	0.37	3.3	150	Break near center, origin near corner, fair mirror
-2	"	0.72	0.27	2.4	100	Break at center, origin 75 μm from corner, good mirror, no branching
-3	"	0.66	0.29	2.6	100	Break at center, origin near corner, good mirror
	Average	0.69	0.31	2.8		

(1) one foot pound hammer

2. Magnesium Dititanate on Silicon Carbide

A magnesium dititanate surface layer was hot pressed at 1200°C on a Norton NC-203 silicon carbide slab as described in the previous section. The magnesium dititanate surface layer did not adhere to the silicon carbide. The other observations for silicon nitride also apply to the silicon carbide specimen.

Attempts were made to cement magnesium dititanate plates to Norton NC-203 silicon carbide using silicate glazes, frits, etc., in an effort to obtain specimens with microcracked surfaces for testing at elevated temperatures. These experiments were unsuccessful.

C. Surfaces with Microcracks Caused by Thermal Expansion Differences between Two Phases

Based upon observations of microcracks in a body consisting of coarse grained silicon carbide in a fine grained matrix of silicon nitride as reported by Lange(22), this combination of materials was selected for investigation. Two methods, hot pressing and sintering, were used in experiments to form these surfaces on hot pressed silicon nitride and silicon carbide.

1. Hot Pressed Surfaces on Silicon Nitride

Several attempts were made to hot press silicon nitride-silicon carbide surface layers on hot pressed Norton HS-130 silicon nitride. 80% by weight of Herman C. Starck silicon nitride powder was mixed with 20% of 400 mesh silicon carbide, together with 5% by weight relative to silicon nitride of MgO added as $MgCO_3$.

Various hot pressing conditions were used, including:

(1) 1650°C at 27.6 MNm^{-2} for 1.5 hours.

(2) 1550°C at 20.7 MNm^{-2} for one hour.

(3) 1500°C at 13.8 MNm^{-2} for 0.75 hours.

At the high temperatures and pressures, the specimens were badly deformed and cracked. Using a graphite retainer and the third set of conditions, the appearance of the slab was good. The thickness of the surface layer was measured and found to be 0.33 mm. Impact bars were cut from the slab and were found to have low impact resistance, apparently due to damage during hot pressing.

In a subsequent experiment, a slab was pressed with the surface layer applied to only one surface, using the third set of conditions again. Specimens cut from this slab and tested with the surface layer on the impact side had impact resistances only as good as the hot pressed controls, and both were lower than as machined controls. Therefore, the attempts to improve the impact resistance of silicon nitride using these hot pressed surface layers have, thus far, been unsuccessful.

2. Hot Pressed Surfaces on Silicon Carbide

Experiments in which silicon carbide-silicon nitride surface layers were formed on silicon carbide by hot pressing were more successful than those reported in the previous section for silicon nitride. Similar procedures and materials were used. 80% by weight silicon nitride and 20% by weight silicon carbide, with 5% MgO added as before, was hot pressed on a slab of Norton NC-203 silicon carbide at 1500°C and 13.8 MNm^{-2} for one hour. The layer was 0.38 mm thick and showed excellent adhesion to the slab. Bars were cut from the slab and the impact resistances were measured with the results shown in Table IX. The impact resistance of the treated specimens was improved, compared with as machined controls.

The fracture surfaces were examined. The most evident feature of these specimens with improved impact resistance, is the tendency to fracture at several places near the center of the span. This type of failure may absorb more energy because of the additional surfaces formed. It is not obvious whether the fracture origins are at the surface or at the interface. In the one case in which a fairly good mirror was observed at the interface, it is possible that the mirror extended into the surface layer, but was not well defined because of the coarse grain size.

In further experiments, four Norton silicon carbide slabs were hot pressed in a single run. Three of these slabs were treated with mixtures of silicon nitride and silicon carbide in the ratios 90-10, 80-20, and 70-30 weight percent. The fourth slab was an as pressed control. The methods and materials were the same as in the previous experiments, except that the Advanced Materials Engineering high alpha phase silicon nitride powder was used. Each slab was placed in its own graphite retainer with graphite foil sprayed with boron nitride powder between the slabs and the graphite separators. The specimens were pressed at 1500°C and 13.8 MNm^{-2} for one hour.

TABLE IX - IMPACT RESISTANCE OF NORTON NC-203 SILICON CARBIDE WITH HOT PRESSED Si_3N_4 - SiC SURFACE LAYERS

Specimen No.	Treatment	Layer Thickness mm	Room Temp. Impact Resistance[1] Joules	in.lbs.	Mirror Radius µm	Comments
JS-31-1	As machined control	--	0.21	1.9	--	
-2	"	--	0.20	1.8	--	
-3	"	--	0.26	2.3	--	
	Average	--	0.22	2.0		
GB-18-1	Hot pressed Si_3N_4-SiC	0.36	0.47	4.1	150	Break at center, origin at edge, poor mirror
-2	"	0.39[2]	0.77	6.8	--	3 breaks at center, origin at corner
-3	"	0.40[2]	0.51	4.5	--	3 breaks at center, origin at corner
-4	"	0.37	0.81	7.2	--	3 breaks at center, origin at corner, poor mirror
	Average	0.38	0.64	5.7		

(1) one foot pound hammer

(2) flawed

The graphite foil adhered strongly to the specimens. Vigorous scraping with a metal spatula was required to remove it. The underlying hot pressed layers showed excellent adherence and abrasion resistance.

The layer-free control slab, as well as the slabs with 90 weight percent and 80 weight percent Si_3N_4, were cracked. The cracks in the layered slabs were mostly curved and ran in a direction roughly paralleling the surface. They originated and terminated at the layer surface or the layer-parent material interface. The cracks in the control slab ran roughly through the center of the slab across the width, but did not transverse the entire thickness.

The 70 weight percent Si_3N_4 powder treated slab cracked in a similar manner as the control slab, but broke into two pieces. The discoloration on the fracture faces indicated the sample cracked at elevated temperature, and the exposed surfaces decomposed or reacted with gases in the die chamber.

None of the bars from this experiment were tested because of the presence of the cracks.

3. Sintering of Silicon Nitride-Silicon Carbide Surfaces

A slip made using the 90% silicon nitride-10% silicon carbide mixture in t-butanol was applied to a slab of Norton NC-203 silicon carbide. These materials were placed in a graphite container and induction heated to 1650°C in 30 minutes and held at that temperature for ten minutes.

The layer formed on the top surface of the slab did not adhere to the slab and was weak and poorly bonded. Under proper conditions, these materials containing MgO should sinter rapidly. Therefore, it is concluded that these conditions caused reactions which interfered with sintering. Oxidation of the silicon nitride or reaction of the silicon nitride with the atmosphere to form a silicon carbide surface layer on the individual silicon nitride particles might prevent the desired sintering.

D. Surfaces with Microcracks Caused by a Phase Transformation

A piece of low elastic modulus zirconia with microcracks caused by the cubic-monoclinic phase transformation was supplied by Professor P. S. Nicholson. ZrO_2 plates, 0.4 and 0.8 mm thick, were cut from this material and

cemented to AVCO silicon nitride bars. The impact resistance of these specimens was measured at room temperature with the results shown in Table X.

An improvement in impact resistance similar to that observed with cemented plates of magnesium dititanate was not observed. The zirconia plates shattered into several pieces rather than crushing, as the magnesium dititanate plates had done. These tests indicate that these zirconia plates were inadequate energy absorbers.

The specimens tested with zirconia plates cemented at the impact point had fracture surfaces that indicated that the fractures occurred at high stresses. In spite of this apparent high stress, the impact resistance was not significantly improved.

E. Vitreous or Semi-Vitreous Surfaces

Vitreous or semi-vitreous surfaces were formed on hot pressed silicon nitride and silicon carbide specimens. A variety of silicate materials were used, including glasses, frits and natural minerals. The descriptions of the surfaces and the impact resistances of the resulting specimens are presented in the following sections.

1. Treatments with Petalite ($LiAlSi_4O_{10}$)

Petalite was applied to the surfaces of silicon nitride and silicon carbide specimens by dipping, spraying and other methods. Spraying was found to be the best method. In early experiments in which petalite was applied to silicon nitride, it was observed that better adhesion was obtained when the specimens were heated under reducing conditions. Poorer adhesion was observed when the specimens were fired under oxidizing conditions in a porcelain muffle. Therefore, in subsequent experiments, the specimens were fired under reducing conditions. The petalite formed a smooth glassy surface after firing at 1400°C for about one hour. After firing at lower temperatures, the material did not mature completely.

AVCO silicon nitride bars were treated with petalite as described above to form surface layers which were about 0.3 mm thick. The impact resistances of the specimens were measured and found to be very low. Examination of the fracture surfaces showed very large fracture mirrors and weak looking fractures. The impact resistances of the fired controls were similar to those of the as machined controls. Therefore, it is evident that flaws were introduced during the treatment which weakened the specimens.

TABLE X

IMPACT RESISTANCE OF AVCO SILICON NITRIDE WITH CEMENTED PLATES OF ZIRCONIA

Specimen No.	Treatment	Layer Thickness mm	Room Temp. Impact Resistance[1] Joules	in.lbs.	Mirror Radius μm	Comments
JSP-23-C1	Control	none	0.27	2.4	---	
-C2	"	none	0.36	3.2	---	
	Average	--	0.32	2.8		
JSP-23-1	Cemented ZrO_2	0.40	0.28[2]	2.5	250	Break at center, origin at corner, fair mirror
-2	"	0.47	0.34[2]	3.0	100	Break near center, origin near edge, good mirror
-3	"	0.83	0.38[2]	3.4	100	Break near center, origin 250 μm from edge, very good mirror
-4	"	0.85	0.33[2]	2.9	200	Break near center, origin at corner, poor mirror
	Average	0.64	0.33	3.0		

(1) one foot pound hammer
(2) the ZrO2 plates shattered into several pieces rather than crushing as the $MgO \cdot 2TiO_2$ plates had done

In the subsequent experiments, a mixture of petalite and 10% ZrO_2 powder was applied to AVCO silicon nitride. Similar results were observed.

After these unsuccessful experiments with silicon nitride, petalite and petalite + 10% ZrO_2 surfaces were formed on Norton silicon carbide. Room temperature impact resistance results are presented in Table XI. Even though improved impact resistance was not observed, the impact resistance did, at least, remain about the same.

There were some features of the fracture surfaces that merit comment. The fracture origins in the petalite treated bars were located at edges of the fracture surfaces, rather than at corners as was typical in the controls. This difference may be caused by healing of corner flaws by the treatment or by the increased stress at the center of the edge caused by the increased thickness of the surface layer at this point. This latter explanation is considered most probable, but it also implies that the flaws at the corners are not as serious as the other evidence might indicate.

There is at least some evidence of higher impact resistance associated with the tendency of the fired controls to fracture at the supports as well as the center of the span.

It was anticipated that the petalite surface layers would be more effective at high temperatures than at room temperature, because the viscosity would be low enough to permit some further deformation which would absorb impact energy. Norton NC-203 silicon carbide and AVCO silicon nitride specimens were treated with petalite and petalite + 10% ZrO_2. The specimens were fired at 1400°C for 45 minutes in a graphite container. The coating thicknesses ranged from about 0.1 to 0.3 mm. The impact resistances of these specimens were measured at 1325°C and results are given in Table XII and XIII. In most cases, the treated specimens had impact resistances two or three times those of the controls. No explanation is available for the low values observed in two cases for Norton NC-203 silicon carbide specimens with petalite + 10% ZrO_2 surface layers. Except for these particular cases, the expected improvement in impact resistance at elevated temperatures was observed.

The fracture surfaces of the treated AVCO specimens are characteristic of specimens with strong fractures, showing that the treatment did not weaken the specimens. The surface of specimen JS-31-CPZET shows an internal flaw (pore or nodule) surrounded by a good, small mirror.

TABLE XI - IMPACT RESISTANCE OF NORTON NC-203 SILICON CARBIDE WITH VITREOUS SURFACE LAYER

Specimen No.	Treatment	Layer Thickness mm	Room Temp. Impact Resistance (1) Joules	in.lbs.	Mirror Radius µm	Comments
JS-31-1	As machined control	--	0.21	1.9	--	
-2	"	--	0.20	1.8	--	
-3	"	--	0.26	2.3	--	
	Average	--	0.22	2.0		
JS-31-1F	Fired control	--	0.46	4.1	375	Break at center and both ends, origin at corner, good mirror
-2F	"	--	0.25	2.2	--	Break at center and one end, possible origin at corner
-3F	"	--	0.30	2.6	--	Break at center and one end, origin at corner, poor mirror
	Average	--	0.34	3.0		
JS-31-1P	Petalite	0.30	0.26	2.3	175	Break at center, origin at edge, fair mirror
-2P	"	0.34	0.22	1.9	--	Break at center, origin at edge, large irregular mirror
-3P	"	0.24	0.22	2.0	200	Break near center, origin at edge, fair mirror
	Average	0.29	0.23	2.1		
JS-31-1PZ	Petalite + 10% ZrO_2	0.16	0.23	2.0	200	Break near center, origin at edge, good mirror
-2PZ	"	0.14	0.31	2.7	200	Break near center, origin at edge, good mirror
-3PZ	"	0.25	0.32	2.8	250	Break near center, origin at edge, good mirror
	Average	0.18	0.29	2.5		

(1) one foot pound hammer

TABLE XII

ELEVATED TEMPERATURE IMPACT RESISTANCE OF AVCO SILICON NITRIDE WITH VITREOUS SURFACE LAYERS
(6.4 x 6.4 x 57 mm bars)

Specimen No.	Treatment	Layer Thickness mm	1325°C Impact Resistance[1] Joules	in. lbs.	Mirror Radius µm	Comments
JS-31-AET	As cut control	--	0.67	5.6	--	
-BET	"	--	0.52	4.6	--	
-CET	"	--	0.45	4.0	--	
	Average	--	0.55	4.7		
JS-31-APET	Petalite	0.26	1.29	11.4	200	Break at center, origin at corner, poor mirror
-BPET	"	0.26	>1.36	>12	--	Did not fracture
-CPET	"	0.22	1.27	11.2	200	Break at center and one end, origin at corner, poor mirror
	Average	0.25	1.28[2]	11.3[2]		
JS-31-APZET	Petalite + 10% ZrO_2 by weight	0.24	>1.36	>12	--	Did not fracture
-BPZET	"	0.16	1.05	9.3	--	Break near center, origin at corner, very poor mirror
-CPZET	"	0.16	1.28	11.3	125	Break near center, origin 250 µm from edge, good mirror
	Average	0.19	1.16[2]	10.3[2]		

(1) one foot pound hammer
(2) two values averaged

TABLE XIII

ELEVATED TEMPERATURE IMPACT RESISTANCE OF NORTON NC-203 SILICON CARBIDE WITH VITREOUS SURFACE LAYERS (6.4 x 6.4 x 57 mm bars)

Specimen No.	Treatment	Layer Thickness mm	1325°C Impact Resistance[1] Joules	in. lbs.	Mirror Radius µm	Comments
JS-31-1ET	As cut control	--	0.25	2.2	--	
-2ET	"	--	0.72	6.4	--	
-3ET	"	--	0.50	4.4	--	
	Average	--	0.49	4.3		
JS-31-PET1	Petalite	0.31	1.28	11.4	200	Break at center, origin at edge, fair mirror
-PET2	"	0.20	1.29	11.4[2]	--	Break at center and one end, possible origin at corner, poor mirror
-PET3	"	0.32	1.03	9.2	250	Break at center, origin at corner, fair mirror
	Average	0.28	1.20	10.7		
JS-31-1PZET	Petalite +10% ZrO_2 by weight	0.13	0.30	2.6	--	Break at center, origin at corner, poor mirror
-2PZET	"	0.10	0.35	3.1	--	Break at center and one end, origin at corner, large mirror
-3PZET	"	0.09	1.19	10.5[2]	200	Break at center, origin at edge, good mirror
	Average	0.11	0.33	2.9[3]		

(1) one foot pound hammer
(2) hammer jammed
(3) average of two test results

Compared with the controls at elevated temperature, the treated Norton NC-203 specimens with higher impact resistance had stronger appearing fracture surfaces with small fracture mirrors. The two treated specimens having low impact resistance had fracture surfaces that differed little, if at all, from those of the specimens that yielded higher values.

The impact resistance of Norton NC-203 silicon carbide specimens with petalite surfaces was investigated at other elevated temperatures. The specimens were fired at 1400°C for 45 minutes in a graphite container. The average thickness of the surface layer was about 0.23 mm. The impact resistances of the treated specimens are given in Table XIV and are compared with appropriate controls in Figure 6, p. 42. Above 1100°C, the impact resistances of the treated specimens increase substantially compared with the controls.

The room temperature impact fractures of specimens treated to form petalite surface layers tend to originate at edges. This tendency was also noted in earlier experiments. However, at elevated temperatures, the fracture origins revert to corners, as is typical of controls. No definite explanation of this variation is available at present.

The specimens that survived the impact without fracturing were examined. As expected, an indentation in the surface was observed. One of these indentations in an AVCO silicon nitride specimen with a petalite surface is illustrated in Figure 7.

In an effort to determine the extent of any interaction between Si_3N_4 samples and layers of petalite applied, one of the pieces of an impact specimen, JS-31-CPET, was cut in cross section and polished. Scans across the petalite, petalite-Si_3N_4 interface, and Si_3N_4 body with an electron probe microanalyzer showed that there was an apparent diffusion of Al into the Si_3N_4 from the petalite over a 12 μm region from the interface. While it was only a small increase, .16% from a constant of .08%, longer treatment times (and perhaps higher temperatures, if feasible) might create an environment for the formation of SIALON solid solutions, which might improve the surface properties and enhance the material's impact resistance.

TABLE XIV

ELEVATED TEMPERATURE IMPACT RESISTANCE OF NORTON NC-203[1] SILICON CARBIDE WITH PETALITE TREATMENT

Specimen No.	Test Temp. °C	1325°C Impact Resistance[2] Joules	1325°C Impact Resistance[2] in.lbs.	Mirror Radius µm	Comments
JS-53-1	25	0.24	2.1	--	Break at center, origin at edge, poor mirror
-2	"	0.16	1.4	250	Break at center, origin at edge, poor mirror
-3	"	0.15	1.3	250	Break near center, origin at edge, fair mirror
	Average	0.18	1.6		
JS-53-4	1100	0.29	2.6	--	Break near center, origin at corner, poor mirror
-5	"	0.38	3.4	250	Break near center, origin at corner, fair mirror
-6	"	0.36	3.2	250	Break off center, origin at corner, fair mirror
	Average	0.35	3.1		
JS-53-7	1200	0.51	4.5	250	Break near center, origin at corner, poor mirror
-8	"	0.47	4.2	--	Break at center, origin at corner, poor mirror
-9	"	0.77	6.8	--	Break at center and one end, origin uncertain
	Average	0.59	5.2		
JS-53-10	1325	0.85	7.5	250	Break at center, origin at corner, poor mirror
-11	"	0.96	8.5	250	Break at center, origin at edge, poor mirror
-12	"	>1.36	>12	--	Did not fracture
	Average	1.05	8.0[3]		

(1) Billet No. 433646
(2) one foot pound hammer
(3) average of two values

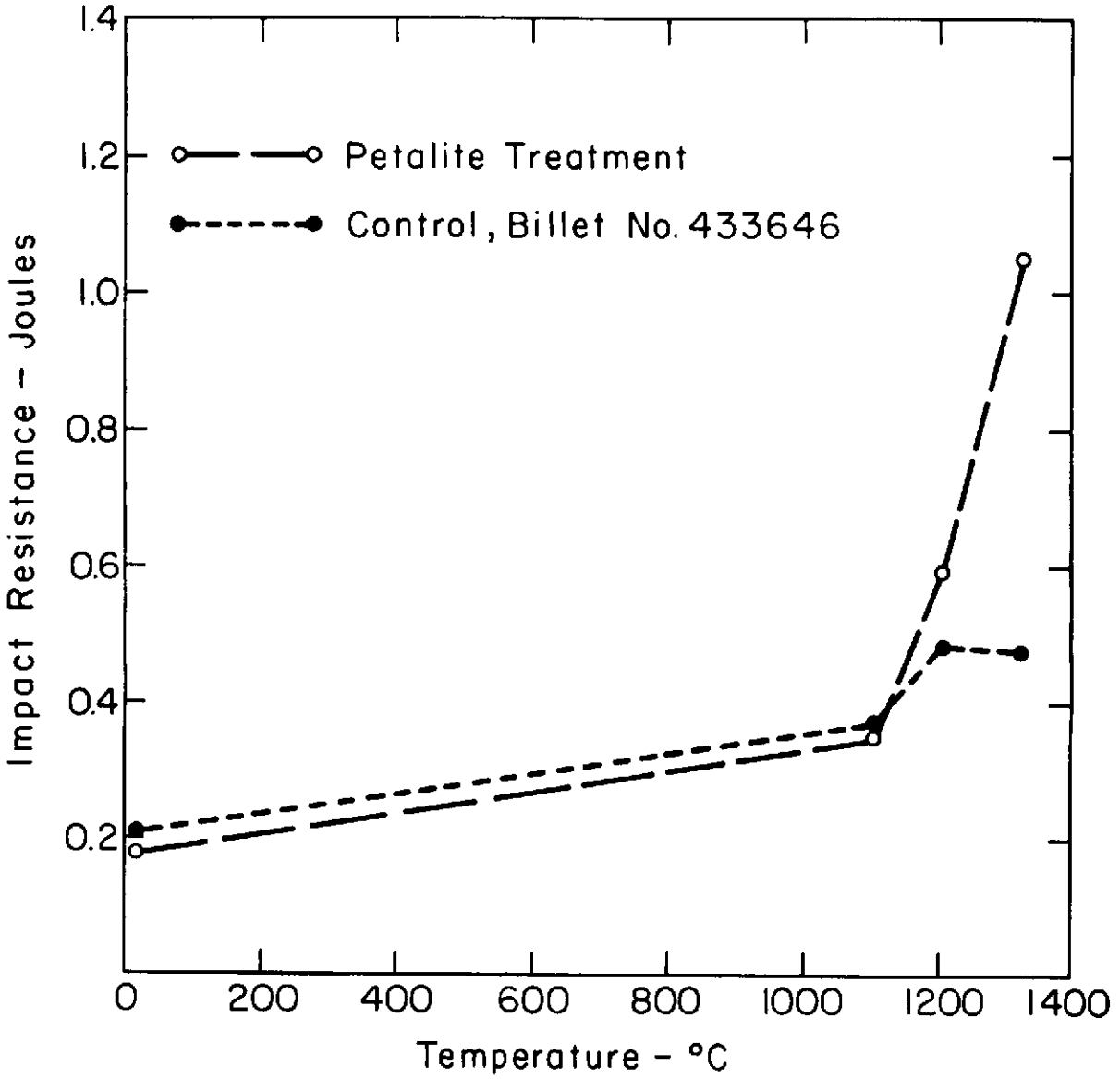

Figure 6 - Impact Resistance vs. Temperature for Norton NC-203 Silicon Carbide

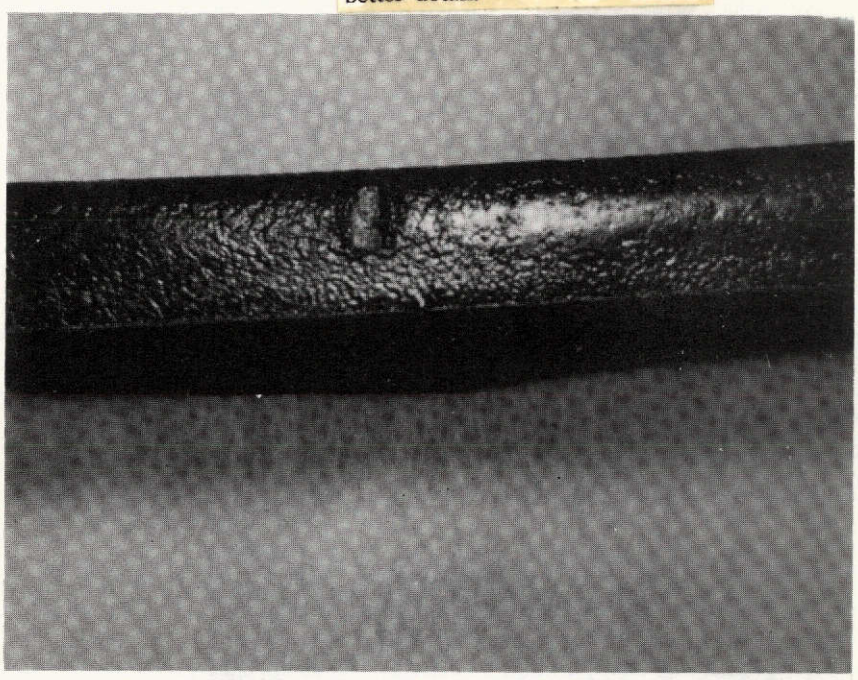

Figure 7 - Surface of AVCO Silicon Nitride Specimen with Petalite Surface, after Impact Testing (Specimen JS-31-BPET)

Specimens with petalite surfaces of various thicknesses and zirconia contents were prepared for burner rig tests. Some of these treated burner rig specimens are illustrated in Figure 8.

2. Treatments with β-spodumene

β-spodumene surface layers were formed on AVCO silicon nitride and fired at 1400°C for 45 minutes in a graphite container. These specimens were unsatisfactory because the viscosity was too low at the firing temperature. The impact resistances of three specimens averaged 0.14 Joules which, when compared with the controls in Table III, indicates that the impact resistance was reduced. Lower firing temperatures (1300° and 1350°C) were used in subsequent experiments, but satisfactory surfaces were not observed.

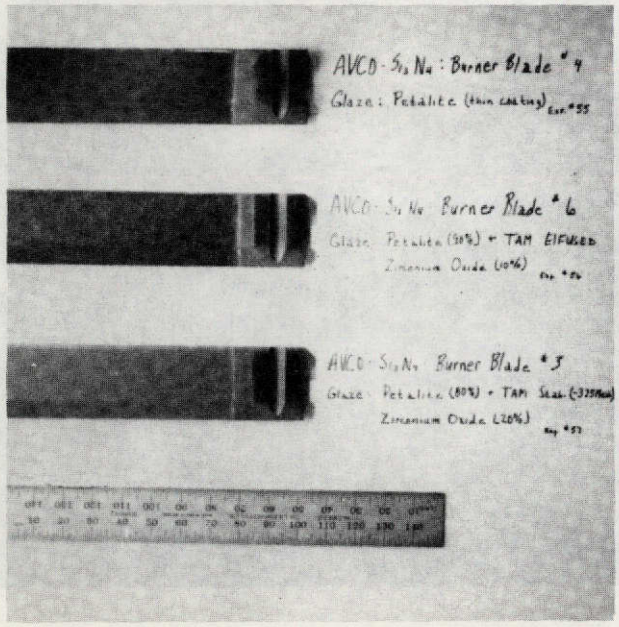

Figure 8 - AVCO Silicon Nitride Burner Rig Specimens with Petalite Surfaces

It is possible to form effective energy absorbing surface layers using the β-spodumene composition as shown by the earlier work at AVCO(2). The starting materials may have been mixed oxides rather than the minerals. This difference may cause the different results in the two cases.

3. Treatments with G-24 Frit

Surface layers about 0.13 mm thick were obtained by spraying the G-24 frit on Norton HS-130 silicon nitride and firing at 1200°C for 15 minutes. 10% ZrO_2 was added to the frit in some cases to increase the viscosity of

the surface layer at elevated temperatures. The results of impact tests are reported in Table XV. The impact resistance of the treated silicon nitride is improved, compared with both sets of controls. Two observations should be noted:

(1) The surface layer sheared off around the impact region and the supports, indicating that the adherence of the surface layer was not as great as desired.

(2) The surface layer tended to become thicker in spots due to effects of surface tension and viscous flow. It is desirable to form thinner surface layers of even thickness.

The fracture mirror measurements do not indicate clearly whether or not the fractures absorbing higher energy occur at higher stresses. However, the treated specimens did, on the average, seem to fracture into a greater number of pieces compared with controls. Also, the fractures in the treated specimens seemed to form better mirrors.

AVCO silicon nitride specimens were treated with G-24 frit in an attempt to improve adherence. The specimens were fired at 1200°C for 15 minutes under reducing conditions. The appearance of the specimens seemed improved, compared with previous experiments, but when the specimens were struck with a hammer, the surface layer came off and was pulverized.

In a further attempt to improve the adhesion of the G-24 frit to Si_3N_4 upon room temperature impact, two methods were tried. The first was to pretreat AVCO Si_3N_4 with a layer of petalite and then treat over this with the G-24 frit. The second was to mix the G-24 frit and petalite in a 2:1 ratio and treat Si_3N_4 with this. It was hoped to obtain the good adhesion properties of the petalite with the apparent energy absorption properties of the G-24 frit. The result in these cases was a clear surface layer which sheared off on impact.

Vitreous surfaces were also formed on Norton NC-203 silicon carbide using G-24 frit. The specimens were fired at 1200°C for 15 minutes under reducing conditions. The G-24 frit did not wet the silicon carbide.

TABLE XV - IMPACT RESISTANCE OF NORTON HS-130 SILICON NITRIDE TREATED WITH G-24 FRIT

Specimen No.	Treatment	Room Temp. Impact Resistance (1) Joules	in. lbs.	Mirror Radius μm	Comments
JSP-24-C1	As cut control	0.40	3.5	--	
-C2	"	0.29	2.6	--	
	Average	0.35	3.1		
JSP-24-CF1	Fired control	0.28	2.5	200	Break near center, origin at corner, poor mirror
-CF2	"	0.28	2.5	175	Break at center, origin at corner, poor mirror
	Average	0.28	2.5		
JSP-24-G1	G-24 frit	0.72	6.4	100	Break near center, origin 250 μm from edge, very good mirror
-G2	"	0.63	5.6	175	Break at center, origin at edge, good mirror
-G3	"	0.27	2.4	300	Break at center, origin near corner, large mirror
	Average	0.54	4.8		
JSP-24-GZ1	G-24 frit + 10% ZrO_2	0.61	5.4	--	Break near center, origin at corner, poor mirror
-GZ2	"	0.36	3.2	150	Break at center, origin near corner, fair mirror
-GZ3	"	0.93	8.2	250	Several breaks near center, origin at corner, good mirror
	Average	0.63	5.6		

(1) one foot pound hammer

4. Other Treatments

Silicon nitride and silicon carbide specimens were treated with a wide variety of other materials in efforts to form vitreous or semi-vitreous surfaces. Among the materials used were vitreous silica, commercially available lithium aluminum silicate glazes, B_2O_3, and a commercially available low expansion borosilicate glass. Various problems were encountered, such as lack of adherence, failure to mature at reasonable temperatures, bubbling, etc. Even though these experiments were unsuccessful, it is likely that by continuing these investigations, methods could be found to demonstrate improved impact resistance using many of these materials.

F. Other Surface Treatments

In other investigations, low expansion surface layers formed by reaction of ceramic bodies with volatile powders have been used to improve the strength of a variety of different types of ceramic bodies. It is likely that similar techniques could be used to treat silicon nitride and silicon carbide. The treatments may form compressive surface layers or energy absorbing surface layers. Norton silicon nitride* cylindrical rods that were packed in Alumina** + 10% aluminum fluoride***, Cr_2O_3****, and spinel***** were fired at 1400°C for two hours. The flexural strengths of the specimens were measured by four point loading on a one inch span and are reported in Table XVI.

The results show that the treated specimens are weaker than the controls. Based upon the earlier results for specimens treated at 1400°C, it seems possible that some of the difficulty is caused by degradation of the silicon nitride during treatment, rather than by any effect of the surface layer.

---

*Norton SN 0404 73A1.

**Alcoa A-15.

***Allied Chemical $Al_2F_6xH_2O$, reagent grade, Code 1232.

****McGean technical grade Cr_2O_3.

*****Muscle Shoals Electrochemical Corp. spinel ($MgAl_2O_4$), Grade 60F.

TABLE XVI

FLEXURAL STRENGTH OF NORTON SILICON NITRIDE
PACKED IN VARIOUS POWDERS

Specimen No.	Packing Materials	Flexural Strength MNm^{-2}	psi
1	Al_2O_3+10% $Al_2F_6 \cdot xH_2O$	596	86,400
2	"	507	73,500
	Average	552	80,000
1	Cr_2O_3	412	59,800
2	"	422	61,200
	Average	417	60,500
1	Spinel	513	74,400
2	"	359	52,000
	Average	436	63,200
1	As machined control	491	71,200
2	"	698	101,200
	Average	595	86,200
A	As machined control	747	108,500
B	"	977	141,700
C	"	800	116,000
	Average	841	122,100

All of the surfaces seem altered by the treatment. A rather thick layer of Cr_2O_3 was formed on the specimens packed in Cr_2O_3. These layers may have energy absorbing surfaces.[3] Therefore, standard bar specimens were packed in spinel and Cr_2O_3 and fired at 1400°C for one hour. The shorter time was chosen in an effort to minimize the previously observed degradation in the strength.

The bars packed in spinel showed some surface alteration. Also, two of the bars were smaller, which indicated possible evaporation. The bars packed in chromium oxide developed a double surface layer. The outer layer was coarse grained with poor adhesion. The inner layer was continuous, glossy and fine grained, and exhibited good adhesion. Upon impact, much of the outer layer came off as a powder, while the inner layer adhered to the Si_3N_4 surface. The impact data are given in Table XVII. The data show there was a small improvement for Cr_2O_3 packed specimens, compared with as received Norton silicon nitride controls reported in Section IV-A.

TABLE XVII

IMPACT RESISTANCE OF NORTON SILICON NITRIDE
PACKED IN VARIOUS POWDERS

Specimen No.	Packing Material	Layer Thickness mm	Room Temp. Impact Resistance[1] Joules	in. lbs.
GB-21-1S	Spinel	negligible	0.49	4.3
-2S	"	negligible	0.30	2.6
-3S	"	negligible	0.32	2.8
	Average	--	0.37	3.3
GB-21-4C	Cr_2O_3	0.23	0.48	4.3
-5C	"	0.23	0.44	3.9
-6C	"	0.24	0.48	4.2
	Average	0.23	0.47	4.1

(1) One foot pound hammer

V. CONCLUSIONS

In this investigation, energy absorbing surface layers were used to improve the impact resistance of silicon nitride and silicon carbide ceramics. The principal conclusions are as follows:

(1) Magnesium dititanate layers cemented on hot pressed silicon nitride specimens resulted in substantial improvements in impact resistance at room temperature. These layers contain microcracks caused by thermal expansion anisotropy and crush on impact, thus yielding improved impact resistance.

(2) Hot pressed silicon nitride-silicon carbide surface layers on hot pressed silicon carbide resulted in a substantial improvement in impact resistance at room temperature. The surface layer material was chosen based on the assumption that microcracks formed as a result of thermal expansion differences between the silicon nitride and the silicon carbide, but the existence of these microcracks was not determined.

(3) Petalite surface layers on silicon carbide and silicon nitride resulted in substantial improvement in impact resistance at elevated temperature. This improvement is attributed to viscous flow of the surface layer material on impact.

VI. REFERENCES

1. T. A. Bragdon, "Evaluation of Cermets for Jet Engine Turbine Blading," WADC Tech. Report 55-215 (January, 1955).

2. W. H. Rhodes and R. M. Cannon, Jr., "High Temperature Compounds for Turbine Vanes," AVCO Systems Division Report, NASA CR-120966, Contract NAS3-14333 (September, 1972).

3. D. R. Platts, H. P. Kirchner and R. M. Gruver, "Strengthening Oxidation Resistant Materials for Gas Turbine Applications," Ceramic Finishing Company Summary Report, NASA CR-121002, Contract NAS3-15561 (September, 1972).

4. A. L. Sutton and V. C. Howard, "The Role of Porosity in the Accommodation of Thermal Expansion in Graphite," J. Nucl. Mat. 7(1) 58-71 (1962).

5. W. R. Buessem, N. Thielke and R. Sarakauskas, "Thermal Expansion Hysteresis of Aluminum Titanate," Ceramic Age 60 (5) 38-40 (1952).

6. W. R. Buessem and F. F. Lange, "Residual Stresses in Anisotropic Ceramics," Interceram 15 (3) 229-231 (1966).

7. B. Morosin and R. W. Lynch, "Structure Studies on Al_2TiO_5 - at Room Temperature and at 600°C," Acta Cryst. B28 (4) 1040-1046 (1972).

8. E. A. Bush and F. A. Hummel, "High Temperature Mechanical Properties of Ceramic Materials: I, Magnesium Dititanate," J. Amer. Ceram. Soc. 41 (6) 189-195 (June, 1958).

9. J. A. Kuszyk and R. C. Bradt, "Influence of Grain Size on Effects of Thermal Expansion Anisotropy in $MgTi_2O_5$," J. Amer. Ceram. Soc. 56 (8) 420-423 (August, 1973).

10. R. V. Sarakauskas, "A Study of Compounds Isomorphous with Aluminum Titanate," M.S. Thesis, The Pennsylvania State University (1952).

11. F. R. Charvat and W. D. Kingery, "Thermal Conductivity, XIII," J. Amer. Ceram. Soc. 40 (9) 306-15 (1959).

12. H. P. Kirchner and R. M. Gruver, "Strength-Anisotropy-Grain Size Relations in Ceramic Oxides," J. Amer. Ceram. Soc. 53 (5) 232-235 (May, 1970).

13. I. Corvin and L. Cartz, "Anisotropic Thermal Expansion of V_2O_5," J. Amer. Ceram. Soc. 48 (6) 328-329 (June, 1965).

14. W. R. Manning, et. al., "Thermal Expansion of Nb_2O_5," J. Amer. Ceram. Soc. 55 (7) 342-347 (July, 1972).

15. H. P. Kirchner and R. M. Gruver, "Strengthening Oxides by Reduction of Crystal Anisotropy," Ceramic Finishing Company Technical Report No. 5, Contract N00014-66-C0190 (April, 1971).

16. R. L. Coble, "Effect of Microstructure on the Mechanical Properties of Ceramic Materials," from Ceramic Fabrication Processes, W. D. Kingery, Editor, John Wiley and Sons, New York, p. 219 (1958).

17. E. A. Bush, "Influence of Crystal Anisotropy on Mechanical Properties of Single Phase Ceramic Materials," Ph.D. Thesis, The Pennsylvania State University, (1958).

18. E. A. Bush and F. A. Hummel, "High Temperature Mechanical Properties of Ceramic Materials: II-β-Eucryptite," J. Amer. Ceram. Soc. 42 (8) 388-391 (August, 1959).

19. R. C. Rossi, "Thermal Shock Resistant Materials," from Ceramics in Severe Environments, Materials Science Research, Volume 5, Edited by W. Kriegel and H. Palmour III, Plenum Press, New York, 123-136 (1971).

20. R. C. Rossi, "Thermal Expansion of BeO-SiC Composites," J. Amer. Ceram. Soc. 52 (5) 290-291 (May, 1969).

21. F. F. Lange, "Effect of Microstructure on Strength of Si_3N_4-SiC Composite System," J. Amer. Ceram. Soc. 56 (9) 445-450 (September, 1973).

22. R. C. Garvie and P. S. Nicholson, "Structure and Thermomechanical Properties of Partially Stabilized Zirconia in the CaO-ZrO_2 System," J. Amer. Ceram. Soc. 55 (3) 152-157 (March, 1972).

23. D. J. Green, P. S. Nicholson and J. D. Embury, "Microstructural Development and Fracture Toughness of a Calcia Partially Stabilized Zirconia," Fracture Mechanics of Ceramics, Vol. 2, Edited by R. C. Bradt, D. P. H. Hasselman and F. F. Lange, Plenum Press, New York (1974) pages 541-553.

24. R. W. Davidge and D. C. Phillips, "The Significance of Impact Data for Brittle Non-Metallic Materials," J. Mat. Sci. 7 (11) 1308-1314 (November, 1972).

25. R. C. Lueth, "An Analysis of Charpy Impact Testing as Applied to Cemented Carbide," presented at the ASTM Symposium, Instrumentive Impact Testing (May, 1973).

26. H. P. Kirchner and R. M. Gruver, "Quantitative Methods for Analysis of Fracture Surfaces in Polycrystalline Ceramics," Ceramic Finishing Company Technical Report No. 7, Contract N00014-66-C0190 (May, 1973).

27. A. Dinsdale, A. J. Moulson and W. T. Wilkinson, "Experiments on Impact Testing of Cylindrical Ceramic Rods," Trans. Brit. Ceram. Soc. 61, 259-275 (1962).

28. J. P. Ashford and E. K. Priddle, The Influence of Specimen Geometry and Structure on the Impact Resistance of Silicon Carbide," Powder Metallurgy 12 (23) 169-192 (1969).